

# Color superconductivity vs. pseudoscalar condensation in a three-flavor NJL model

Harmen J. Warringa and Daniël Boer

*Department of Physics and Astronomy, Vrije Universiteit,  
De Boelelaan 1081, 1081 HV Amsterdam, The Netherlands\**

Jens O. Andersen

*Nordita, Blegdamsvej 17, DK-2100 Copenhagen Ø, Denmark†*

(Dated: October 24, 2018)

We calculate numerically the phase diagram of the three-flavor Nambu–Jona-Lasinio model at zero and finite temperature as a function of the up, down, and strange quark chemical potentials. We focus on the competition between pseudoscalar condensation and color superconductivity. We find that the two types of phases are separated by first-order transitions.

## I. INTRODUCTION

In recent years a huge effort has been made in order to understand the phase diagram of strongly interacting matter, both experimentally as well as theoretically. Collisions at the Relativistic Heavy-Ion Collider (RHIC) at BNL and the Large Hadron Collider (LHC) at CERN allow the experimental study of hadronic matter at energy densities exceeding that required to create a quark-gluon plasma. The energy and baryon densities of these experiments correspond to temperatures up to 200 MeV and a baryon chemical potential in the range 0–600 MeV.

At zero baryon chemical potential, lattice calculations suggest the existence of a transition from ordinary nuclear matter to a quark-gluon plasma at temperatures of around 160 MeV (see for example Ref. [1]). While there has been progress in generalizing lattice calculations to finite baryon chemical potential [2, 3, 4, 5], highly nontrivial problems remain to be solved, and in practice one is restricted to small baryon chemical potentials.

Since one cannot apply lattice gauge theories to the region of the phase diagram where the baryon chemical potential is large, one must employ other methods. One possibility is perturbative QCD. Asymptotic freedom guarantees that this method can be applied at asymptotically large chemical potentials. If the densities are too small to use perturbative QCD, one may apply effective theories. Models such as the instanton liquid model, random matrix models, and Nambu–Jona-Lasinio (NJL) models have been applied to the study of the QCD phase diagram at finite temperature and densities. Despite their shortcomings, it is expected that such models do describe the qualitative features of the QCD phase diagram, in regions not accessible to perturbative or lattice QCD. For example, the existence of a critical point at finite baryon chemical potential has been predicted using effective models [6, 7]. Furthermore, it

is expected that quark matter at high baryon chemical potentials and low temperatures can be in a two-flavor color-superconducting phase (2SC) [8, 9, 10] or a color-flavor locked (CFL) phase [11, 12]. In these phases gaps on the order of 100 MeV arise.

Many results have been obtained for equal up, down and strange quark chemical potentials. However, this may not be directly relevant for heavy-ion collisions or compact stars. For example, to enforce electric and color neutrality and weak equilibrium in compact stars different flavor and color chemical potentials have been introduced [13, 14]. This gives rise to a more complicated phase diagram in which one also finds new 2SC-like [15] and gapless superconducting phases [16, 17, 18, 19, 20, 21, 22, 23]. Similarly, in heavy-ion collisions, a difference between the quark chemical potentials arises if the number densities of the different quark flavors are not the same. This difference can cause interesting observable effects such as two critical end-points [24, 25]. However, instanton induced interactions tend to suppress this effect [26].

In addition to a more complicated structure of the superconducting phases, different chemical potentials can also trigger pseudoscalar condensation [27, 28, 29]. This has been confirmed on the lattice at zero baryon but finite isospin chemical potential [30]. Depending on the flavors involved, the charged pion, neutral or charged kaon fields may acquire a vacuum expectation value. Pseudoscalar condensation in the two-flavor NJL model has been studied in Refs. [25, 31], as a function of the different chemical potentials at zero and finite temperature. An extension to three flavors was carried out in Ref. [32].

In this paper, we discuss the phase diagram of the three-flavor NJL model as a function of the different chemical potentials including both pseudoscalar condensation and color superconductivity. We did not apply electric or color neutrality conditions. At zero temperature, pseudoscalar condensation is possible if  $|\mu_u - \mu_d| > m_\pi$  [27] or if  $|\mu_{u,d} - \mu_s| > m_K$  [28]. On the other hand, color superconducting phases occur if the chemical potentials are large and approximately equal. Therefore, one can imagine scenarios where for example  $\mu_u \approx \mu_d$  (the

\*Electronic address: harmen@nat.vu.nl, dboer@nat.vu.nl

†Electronic address: jensoa@nordita.dk

Fermi surfaces of the  $u$  and  $d$  quark should be sufficiently close for Cooper pairing to occur) and  $\mu_u \approx -\mu_s$  (the Fermi surfaces of the  $u$  and  $\bar{s}$  should be sufficiently close for kaon condensation to occur), with  $|\mu_{u,d} - \mu_s| > m_K$ . In such a case a 2SC phase is competing against a phase in which kaons condense. From our calculations it follows that a coexistence phase of pseudoscalar condensation and color superconductivity does not occur for the parameters chosen and that these phases are separated by a first-order transition. However, we do not exclude that other choices of parameters may lead to such a coexistence phase, just as coexistence of color superconductivity and chiral symmetry breaking may occur in the NJL model for specific ranges of parameters [33]. Here we refer to a coexistence phase to mean a phase in which two condensates are nonzero simultaneously.

In this work we study pseudoscalar condensation in the quark anti-quark channel. We have not taken into account the pseudoscalar diquark interaction. This interaction is suppressed relative to the scalar diquark interaction due to instantons [10]. However in absence of instanton interactions, if one neutralizes the bulk matter with respect to color and electric charges it is possible to have pseudoscalar diquark condensation with rather large gaps [34]. Pseudoscalar diquark condensation in the NJL model is similar [34] to pseudoscalar condensation in the CFL phase studied with effective chiral models in Refs. [35, 36, 37, 38, 39, 40, 41].

We emphasize that in this paper we do not impose electric or color neutrality conditions, but that this would qualitatively affect the phase structure, leading for example to the observation that in a macroscopic volume of quark matter the 2SC phase is energetically disfavored [13, 14]. Therefore, our results do not address the qualitative features of the QCD phase structure with neutrality constraints imposed.

The paper is organized as follows. In Sec. II, we briefly describe the NJL model and the choice of parameters. In Sec. III, we discuss the calculations and some of its technical aspects. In Sec. IV, we present our results, and in Sec. V we conclude.

## II. THE NJL MODEL

In the NJL model [42], one treats the interaction between the quarks as a point-like quark color current-current interaction. This naive approximation to QCD works very well in explaining various low-energy observables such as hadron masses [43]. By applying several Fierz transformations to the current-current interaction (see for example Ref. [44]) and including only terms which give rise to attractive  $qq$  and  $\bar{q}q$  channels, one obtains the following Lagrangian density

$$\mathcal{L} = \bar{\psi} (i\gamma^\mu \partial_\mu - M_0 + \mu\gamma_0) \psi + \mathcal{L}_{\bar{q}q} + \mathcal{L}_{qq}, \quad (1)$$

where the quark-antiquark term,  $\mathcal{L}_{\bar{q}q}$ , and the diquark interaction term,  $\mathcal{L}_{qq}$ , are defined below. We have sup-

pressed the color, flavor, and Dirac indices of the fermion fields  $\psi$  for notational simplicity. The mass matrix  $M_0$  is diagonal and contains the bare quark masses  $m_{0u}$ ,  $m_{0d}$  and  $m_{0s}$ . The matrix  $\mu$  is also diagonal and contains the quark chemical potentials  $\mu_u$ ,  $\mu_d$  and  $\mu_s$ . We use the metric  $g^{\mu\nu} = \text{diag}(+ - - -)$  and the standard representation for the  $\gamma$ -matrices. The quark-antiquark interaction part of the Lagrangian density is

$$\mathcal{L}_{\bar{q}q} = G \left[ (\bar{\psi} \lambda_a \psi)^2 + (\bar{\psi} \lambda_a i\gamma_5 \psi)^2 \right]. \quad (2)$$

The matrices  $\lambda_a$  are the 9 generators of U(3) and act in flavor space. They are normalized as  $\text{Tr} \lambda_a \lambda_b = 2\delta_{ab}$ . The diquark interaction term of the Lagrangian density is given by

$$\mathcal{L}_{qq} = \frac{3}{4} G (\bar{\psi} t_A \lambda_B C i\gamma_5 \bar{\psi}^T) (\psi^T t_A \lambda_B C i\gamma_5 \psi), \quad (3)$$

where  $A, B \in \{2, 5, 7\}$  since only the interaction in the color and flavor antisymmetric triplet channel is attractive. The matrices  $t_a$  are the generators of U(3) and act in color space. Their normalization is  $\text{Tr} t_a t_b = 2\delta_{ab}$ . To remind the reader, the antisymmetric flavor matrices  $\lambda_2$ ,  $\lambda_5$  and  $\lambda_7$  couple up to down, up to strange and down to strange quarks, respectively. The charge conjugate of a field  $\psi$  is denoted by  $\psi_c = C\bar{\psi}^T$  where  $C = i\gamma_0\gamma_2$ . The coupling strength  $3G/4$  of the diquark interaction is fixed by the Fierz transformation. However, some authors discuss the NJL model with a different diquark coupling constant (see for example Ref. [22] for a comparison).

The results that will be presented below are obtained with the following choice of parameters

$$m_{0u} = m_{0d} = 5.5 \text{ MeV}, \quad m_{0s} = 112 \text{ MeV} \\ G = 2.319/\Lambda^2, \quad \Lambda = 602.3 \text{ MeV}. \quad (4)$$

This choice of parameters gives rise to constituent quark masses  $M_u = M_d = 368 \text{ MeV}$  and  $M_s = 550 \text{ MeV}$  [44].

## III. THE EFFECTIVE POTENTIAL

To obtain the phase diagram of the NJL model, we first introduce 18 real condensates  $\alpha_a$  and  $\beta_a$ , and 9 complex condensates  $\Delta_{AB}$  as follows

$$\alpha_a = -2G \langle \bar{\psi} \lambda_a \psi \rangle, \quad (5)$$

$$\beta_a = -2G \langle \bar{\psi} \lambda_a i\gamma_5 \psi \rangle, \quad (6)$$

$$\Delta_{AB} = \frac{3}{2} G \langle \psi^T t_A \lambda_B C \gamma_5 \psi \rangle. \quad (7)$$

We will assume that all condensates are space-time independent. The crystalline Larkin-Ovchinnikov-Fulde-Ferrell (LOFF) phase [45] will not be considered here. The next step is to apply a Hubbard-Stratonovich transformation to eliminate the four-point quark interactions to make the Lagrangian quadratic in the quark fields. Introducing a two-component Nambu-Gorkov field  $\Psi^T =$

$(\psi^T, \psi_c^T)/\sqrt{2}$  allows for straightforward integration over the quark fields. After going to imaginary time, the thermal effective potential  $\mathcal{V}$  in the mean-field approximation reads

$$\mathcal{V} = \frac{\alpha_a^2 + \beta_a^2}{4G} + \frac{|\Delta_{AB}|^2}{3G} - \frac{T}{2} \sum_{p_0=(2n+1)\pi T} \int \frac{d^3p}{(2\pi)^3} \log \det K, \quad (8)$$

where  $K$  is a  $72 \times 72$  matrix

$$K = \begin{pmatrix} \mathbb{1}_c \otimes \mathcal{D}_1 & \Delta_{AB} t_A \otimes \lambda_B \otimes \gamma_5 \\ -\Delta_{AB}^* t_A \otimes \lambda_B \otimes \gamma_5 & \mathbb{1}_c \otimes \mathcal{D}_2 \end{pmatrix}, \quad (9)$$

and

$$\mathcal{D}_1 = \mathbb{1}_f \otimes (i\gamma_0 p_0 + \gamma_i p_i) - \mu \otimes \gamma_0 - (M_0 + \alpha_a \lambda_a) \otimes \mathbb{1}_d - \beta_a \lambda_a \otimes i\gamma_5, \quad (10)$$

$$\mathcal{D}_2 = \mathbb{1}_f \otimes (i\gamma_0 p_0 + \gamma_i p_i) + \mu \otimes \gamma_0 - (M_0 + \alpha_a \lambda_a^T) \otimes \mathbb{1}_d - \beta_a \lambda_a^T \otimes i\gamma_5. \quad (11)$$

The matrix  $\mathbb{1}$  is the identity matrix in color ( $c$ ), flavor ( $f$ ), or Dirac ( $d$ ) space.

The values of the condensates and the phase diagram are determined by minimizing the effective potential  $\mathcal{V}$  with respect to the condensates. To make the minimization procedure easier, one can take advantage of the fact that certain condensates must vanish. Firstly, application of QCD inequalities [27, 46] shows that in QCD at zero chemical potential chiral symmetry breaking cannot be driven by parity-violating condensates of the type  $\langle \psi i \gamma_5 \psi \rangle$ . Outside the phase in which diquarks condense, we found numerically that this is also correct in the NJL model at finite chemical potentials. Therefore,  $\beta_0$ ,  $\beta_3$  and  $\beta_8$  are put to zero. Secondly, although perturbative one-gluon exchange cannot distinguish between  $\beta_k$  and  $\alpha_k$  condensation with  $k \in \{1, 2, 4, 5, 6, 7\}$ , pseudoscalar condensation is favored due to the instanton interaction [27]. We therefore set all  $\alpha_k$ 's with  $k \in \{1, 2, 4, 5, 6, 7\}$  to zero. We found numerically that this is correct, despite the fact that the model we consider does not include instanton interactions.

One can further simplify the minimization procedure by using the symmetries of the NJL model. In absence of quark masses and chemical potentials, the Lagrangian density has a global  $SU(3)_c \times U(3)_V \times U(3)_A$  symmetry. Due to the non-vanishing quark masses, the symmetry is broken down to  $SU(3)_c \times U(3)_V$ . Since we consider different quark masses and finite chemical potentials, the symmetry of the Lagrangian density is further reduced to  $SU(3)_c \times U(1)_u \times U(1)_d \times U(1)_s$ . The vacuum manifold is invariant under the same transformations as the Lagrangian density, so applying a  $U(1)$ -flavor transformation to all condensates leaves the free energy invariant. Therefore, using the  $U(1)$ -flavor transformations one can choose the pseudoscalars to condense in the  $\beta_2$ ,  $\beta_5$ , and  $\beta_7$  channels, and set  $\beta_1$ ,  $\beta_4$  and  $\beta_6$  to zero. The phase in

which  $\beta_2$ ,  $\beta_5$  or  $\beta_7$  is non-vanishing is called the  $\pi^+/\pi^-$ ,  $K^0/\bar{K}^0$  or  $K^+/K^-$  condensed phase, respectively.

Because of the global  $SU(3)_c$  symmetry, one can also rotate away several diquark condensates. Without loss of generality, we can minimize with respect to  $\Delta_{22}$ ,  $\Delta_{25}$ ,  $\Delta_{55}$ ,  $\Delta_{27}$ ,  $\Delta_{57}$  and  $\Delta_{77}$ . In principle, all six diquark condensates can have a phase. It is always possible to remove two of them by using the two diagonal  $SU(3)_c$  transformations. As long as there is no pseudoscalar condensation, one can use the  $U(1)$ -flavor symmetries to rotate away three other phases. As a result either  $\Delta_{25}$ ,  $\Delta_{55}$ ,  $\Delta_{27}$ , or  $\Delta_{57}$  has a phase [44]. However, this reduction is not completely possible if pseudoscalar condensation occurs. By choosing the pseudoscalars to condense in the  $\beta_2$ ,  $\beta_5$  and  $\beta_7$  channels, one breaks the  $U(1)$ -flavor symmetry. Hence if pseudoscalar condensation arises in one channel, one can in general rotate away one phase less in the diquark sector. If it occurs in more channels, two phases less can be rotated away. However, numerically we find that allowing for a complex phase leads to diquark condensation only in the  $\Delta_{22}$ ,  $\Delta_{55}$  and the  $\Delta_{77}$  channels. The  $\Delta_{25}$ ,  $\Delta_{27}$ , and  $\Delta_{57}$  diquark condensates do not arise or can be rotated away. Moreover, we find that pseudoscalar condensation in the quark-antiquark channel does not coexist with color superconductivity, such that one can always take the diquark condensates to be real.

The different possible color-superconducting phases are named as follows [22]

$$\begin{aligned} \Delta_{22} \neq 0, \Delta_{55} \neq 0, \Delta_{77} \neq 0 & \quad \text{CFL}, \\ \Delta_{77} = 0, \Delta_{22} \neq 0, \Delta_{55} \neq 0 & \quad \text{uSC}, \\ \Delta_{55} = 0, \Delta_{22} \neq 0, \Delta_{77} \neq 0 & \quad \text{dSC}, \\ \Delta_{22} = 0, \Delta_{55} \neq 0, \Delta_{77} \neq 0 & \quad \text{sSC}, \\ \Delta_{22} \neq 0, \Delta_{55} = 0, \Delta_{77} = 0 & \quad \text{2SC}, \\ \Delta_{55} \neq 0, \Delta_{22} = 0, \Delta_{77} = 0 & \quad \text{2SCus}, \\ \Delta_{77} \neq 0, \Delta_{22} = 0, \Delta_{55} = 0 & \quad \text{2SCds}. \end{aligned} \quad (12)$$

To calculate the effective potential in an efficient way, one can multiply the matrix  $K$  with  $\text{diag}(\mathbb{1}_c \otimes \mathbb{1}_f \otimes \gamma_0, \mathbb{1}_c \otimes \mathbb{1}_f \otimes \gamma_0)$  which leaves the determinant invariant. In this way, one obtains a new matrix  $K'$  with  $ip_0$ 's on the diagonal. By determining the eigenvalues of the matrix  $K'$  with  $p_0 = 0$ , one can reconstruct the determinant of  $K$  for all values of  $p_0$  which is namely  $\prod_{i=1}^{72} (\lambda_i - ip_0)$ . After summing over Matsubara frequencies, one finds

$$T \sum_{p_0=(2n+1)\pi T} \log \det K = \sum_{i=1}^{72} \left[ \frac{\lambda_i}{2} + T \log \left( 1 + e^{-\lambda_i T} \right) \right]. \quad (13)$$

All that remains in order to determine the effective potential is to integrate over three-momentum  $p$  up to an ultraviolet cutoff  $\Lambda$ .

The speed of the calculation of the effective potential depends heavily on how fast one can compute the eigenvalues. There are several ways to speed up the calculation. Firstly, the determinant of  $K$  does not depend

on the direction of  $\vec{p}$ . Therefore, one can choose  $\vec{p}$  to lie in the  $z$ -direction. Together with the choice of the non-vanishing condensates mentioned above, this implies that  $K'(p_0 = 0)$  becomes a real symmetric matrix, which simplifies the calculation of the eigenvalues. Secondly, one can interchange rows and columns of  $K'$  without changing its determinant. By doing so, one can bring  $K'$  in a block-diagonal form. One can then determine the eigenvalues of the blocks separately which is significantly faster since the time needed to compute eigenvalues numerically scales cubically with the dimension of the matrix. In the most general case with diquark condensation, one can always reduce the problem to two  $36 \times 36$  matrices. Moreover, if there is no diquark condensation, but only pseudoscalar condensation, the problem can be further reduced to computing the eigenvalues of two  $6 \times 6$  matrices.

We determined the eigenvalues using LAPACK routines [47]. After numerical integration over three-momentum  $p$  up to the cutoff, the condensates were determined by minimizing the effective potential using MINUIT [48]. To be certain that the minimization procedure did not end up in a local minimum, we always checked the continuity of the minimized effective potential as a function of chemical potentials and/or temperature.

#### IV. PHASE DIAGRAMS

In this section, we present our results for the phase diagrams of the NJL model with  $u$ ,  $d$ , and  $s$  quarks. We plot the phase diagrams as a function of the chemical potentials and temperature. To determine the locations of the phase boundaries, we examine the behavior of the condensates. If a condensate jumps discontinuously the transition is first-order, and this is indicated by a solid line. If its derivative has a discontinuity, the transition is second order, and this is indicated by a dotted line. If a condensate changes rapidly in a narrow range without vanishing there is a smooth cross-over, and this is indicated by a dashed-dotted line at the point where the condensate varies maximally.

##### A. $\mu_s = 0$ and $T = 0$

In Fig. 1, we display the phase diagram of the NJL model for  $\mu_s = 0$  and  $T = 0$  as a function of  $\mu_u$  and  $\mu_d$ . Outside the 2SC phase (q), our results agree qualitatively with the two-flavor calculations of Ref. [31] (see their Fig. 1), where color-superconducting phases were not taken into account. Moreover, in Ref. [31] different parameters were used, in addition to a form factor which mimics asymptotic freedom.

One can clearly see that the phase diagram is symmetric under reflection in the origin. This is because the free energy is invariant under the transformation

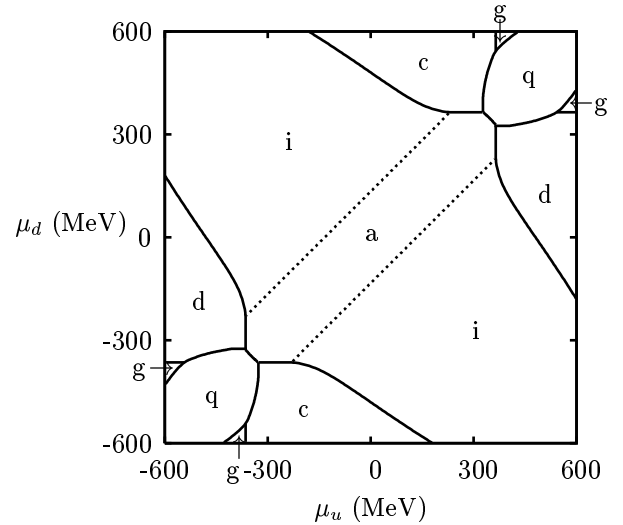


FIG. 1: Phase diagram for  $\mu_s = 0$  and  $T = 0$  as a function of  $\mu_u$  and  $\mu_d$ . First and second-order transitions are indicated by solid and dotted lines, respectively. The letters denote the different phases, where a:  $\bar{u}u + \bar{d}d + \bar{s}s$ , c:  $\bar{u}u + \bar{s}s$ , d:  $\bar{d}d + \bar{s}s$ , g:  $\bar{s}s$ , i:  $\pi^+/\pi^- + \bar{s}s$  and q: 2SC +  $\bar{s}s$ .

$(\mu_u, \mu_d, \mu_s) \rightarrow (-\mu_u, -\mu_d, -\mu_s)$  from the symmetry between particles and anti-particles. Fig. 1 is also symmetric under interchange of  $u$  and  $d$ , because of the choice of equal up and down quark masses. This gives rise to the symmetry of the phase boundaries with respect to the diagonals.

In general, horizontal and vertical lines in the phase diagrams arise if the pairing of one type of quark is not changed after a transition. In this case, the location of the phase boundary is determined by the properties of other quarks. Therefore, changing the chemical potential of the unchanged quark species cannot have a big influence on the location of the phase boundary. This results in the horizontal and vertical lines. For  $T = 0$ , one always finds these lines near the values of the constituent quark masses, i.e.  $\mu_u \approx M_u$ ,  $\mu_d \approx M_d$  and  $\mu_s \approx M_s$  (see for example Ref. [44]). The diagonal lines arise because at  $T = 0$  pion condensation can occur if  $|\mu_u - \mu_d| > m_\pi = 138$  MeV [27].

The diagram shows that if the chemical potentials are different, the transition to the color-superconducting phase (q) remains first order as was concluded in Ref. [49]. Moreover, one can see from Fig. 1 that if  $\mu_u \neq \mu_d$  it is possible to go through two first-order transitions before entering the 2SC phase (q) (similar to the situation discussed in Ref. [25] without color superconductivity). We observe that to have such a scenario at zero temperature, a minimum difference between  $\mu_u$  and  $\mu_d$  is required. In the present case this is about 35 MeV. Pion condensation (i) and the 2SC phase (q) are in this diagram separated by two phase transitions in contrast to the estimated  $(\mu_B, \mu_I)$  phase diagram of Ref. [50].

### B. $\mu_d = 0$ and $T = 0$

In Fig. 2 we display the phase diagram for  $\mu_d = 0$  and  $T = 0$  as a function of  $\mu_u$  and  $\mu_s$ . Since the up and down quark masses are much smaller than the strange quark mass, this diagram is very different from Fig. 1. Besides the possibility of pion condensation in (h) and (i), phases in which the charged kaon (k) and the neutral kaon condense (l)/(m) arise. The lines separating the charged kaon phase (k) from the chirally broken phase (a) are diagonal because at  $T = 0$  kaon condensation can occur if  $|\mu_s - \mu_{u,d}| > m_K = 450$  MeV [28] (the chosen parameter set gives rise to a somewhat low kaon mass, but this is not relevant for the qualitative features of the phase diagram). In (r) we find the 2SCus phase. This phase is surrounded by phases in which the pions (h)/(i) and the neutral kaons (l) condense. We find that one passes a first-order transition when going from the pion and neutral kaon condensed to the 2SCus phase.

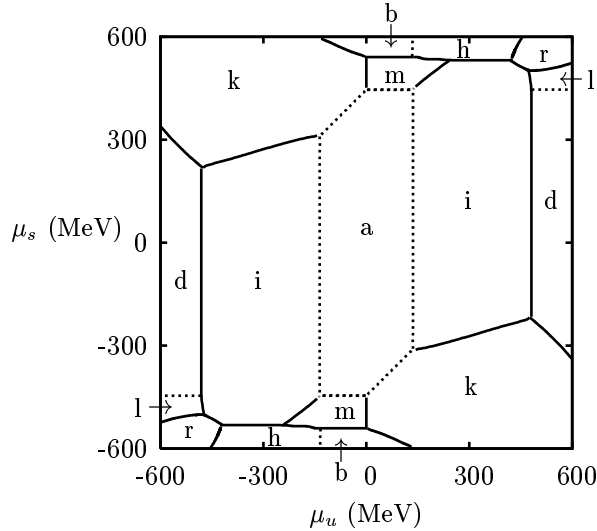


FIG. 2: Phase diagram for  $\mu_d = 0$  and  $T = 0$  as a function of  $\mu_u$  and  $\mu_s$ . First and second-order transitions are indicated by solid and dotted lines, respectively. The letters denote the different phases, where a:  $\bar{u}u + \bar{d}d + \bar{s}s$ , b:  $\bar{u}u + \bar{d}d$ , d:  $\bar{d}d + \bar{s}s$ , h:  $\pi^+/\pi^-$ , i:  $\pi^+/\pi^- + \bar{s}s$ , k:  $K^+/K^- + \bar{d}d$ , l:  $K^0/\bar{K}^0 + \bar{u}u$ , m:  $K^0/\bar{K}^0 + \bar{u}u$  and r: 2SCus +  $\bar{d}d$ .

### C. $\mu_u \approx \mu_d$

In Fig. 3, we display the phase diagram for  $T = 0$  as a function of the up and down quark chemical potential and the strange quark chemical potential. We have chosen  $\mu_u = \mu_d + \epsilon$  where  $\epsilon$  is a very small positive number. This  $\epsilon$  is necessary because when  $\epsilon = 0$  one is just at a first-order phase boundary between the phase in which the charged kaons condense (k) and the one in which the neutral kaons condense (m), as can be seen from Fig. 2. This nonzero value of  $\epsilon$  gives rise to a small asymmetry in

the phase diagram. If  $\epsilon$  is chosen negative, the phases in which the neutral (l)/(m) and the charged (j)/(k) kaon condensates are interchanged.

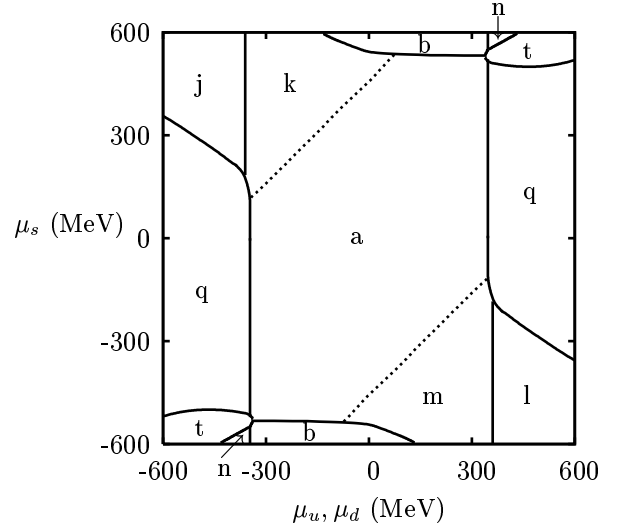


FIG. 3: Phase diagram for  $T = 0$  as a function of  $\mu_u = \mu_d + \epsilon$  and  $\mu_s$ . First and second-order transitions are indicated by solid and dotted lines, respectively. The letters denote the different phases, where a:  $\bar{u}u + \bar{d}d + \bar{s}s$ , b:  $\bar{u}u + \bar{d}d$ , j:  $K^+/K^-$ , k:  $K^+/K^- + \bar{d}d$ , l:  $K^0/\bar{K}^0 + \bar{u}u$ , m:  $K^0/\bar{K}^0 + \bar{u}u$ , n: 2SC, q: 2SC +  $\bar{s}s$  and t: CFL.

Apart from the additional 2SC (n)/(q) and CFL (t) phases, our results agree qualitatively with the three-flavor calculations of Ref. [32] (see their Fig. 7).

The authors of Ref. [32] used different quark masses and a different coupling constant, and in addition employed a form factor to mimic asymptotic freedom. Therefore, one may conclude that the use of such a form factor does not affect the phase diagram qualitatively. We would also like to point out that the phase diagram Fig. 3 cannot simply be obtained by a superposition of phase diagrams obtained from a calculation with pseudoscalar condensation, but without superconductivity (such as done in [32]), and one with superconductivity, but without pseudoscalar condensation (such as done in [51]). Despite the fact that the two types of phases do not coexist, there is nevertheless competition between them. Figure 3 shows that the  $K^0/\bar{K}^0$  (l)/(m) and the  $K^+/K^-$  (j)/(k) phases are separated from the 2SC phase (q) by a first-order transition. This remains the case at finite temperature as is illustrated in Fig. 4. This figure displays the phase diagram as a function of  $\mu_s$  and temperature, for fixed  $\mu_u = \mu_d = 550$  MeV.

Returning to the discussion of Fig. 3; the line  $\mu_u = \mu_d = \mu_s$  goes through the phase (a) in which chiral symmetry is spontaneously broken. At some point it enters via a first-order transition the 2SC +  $\bar{s}s$  phase (q), and finally goes into the CFL phase (t), again via a first-order transition. If there is a difference between  $\mu_u = \mu_d$  and  $\mu_s$ , one can see from Fig. 3 that as the densities increase,

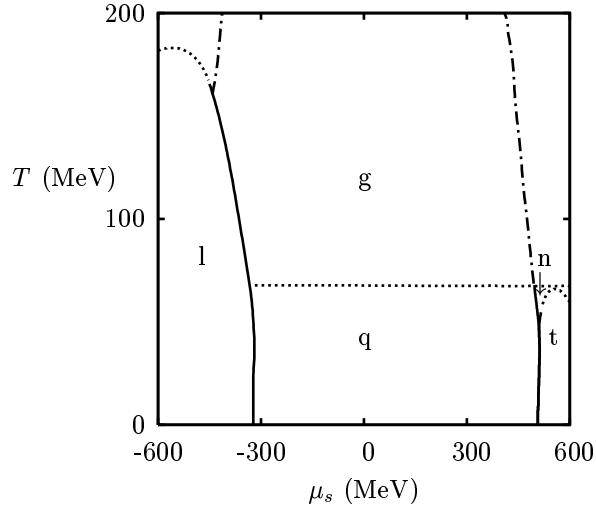


FIG. 4: Phase diagram as a function of  $\mu_s$  and  $T$ , for fixed  $\mu_u = \mu_d = 550$  MeV. First and second-order transitions are indicated by solid and dotted lines respectively, while cross-overs are indicated by dashed-dotted lines. The uppermost phase without label is the restored phase. The letters denote the different phases, where g:  $\bar{s}s$ , l:  $K^0/\bar{K}^0$ , n: 2SC, q: 2SC +  $\bar{s}s$  and t: CFL.

quark matter can go directly from a phase of spontaneous chiral symmetry breaking (a) to a CFL phase (t) without passing the 2SC phase (q) first. This can also occur in compact stars [13]. One should keep in mind though that the relation between chemical potential and number density is not linear. For example, at a first-order phase boundary, the number density increases discontinuously. At these particular densities, quark matter can be in a mixed state of normal and superconducting matter [49, 52].

It is also interesting to note that the phases (l)/(j) of kaon condensation can also occur outside the region of spontaneous chiral symmetry breaking. Assuming the phase transition towards chiral symmetry restoration coincides with the deconfinement transition (as appears to be the case in lattice studies at small baryon chemical potential and in some models), this would imply that condensation of a state with quantum numbers of the kaon may persist in the deconfined phase. This was first observed in Ref. [27], based on a perturbative calculation at high isospin chemical potential, that is expected to be applicable only in the deconfined region.

#### D. $\mu_u = \mu_s$

In Fig. 5, we show the phase diagram at zero temperature as a function of  $\mu_u = \mu_s$  and  $\mu_d$ . This diagram is similar to Fig. 1 for small strange quark chemical potentials (below the kaon mass). At larger strange quark chemical potentials the diagrams differ, exhibiting kaon condensation (l) and diquark condensation involv-

ing strange quarks (r)/(o)/(t).

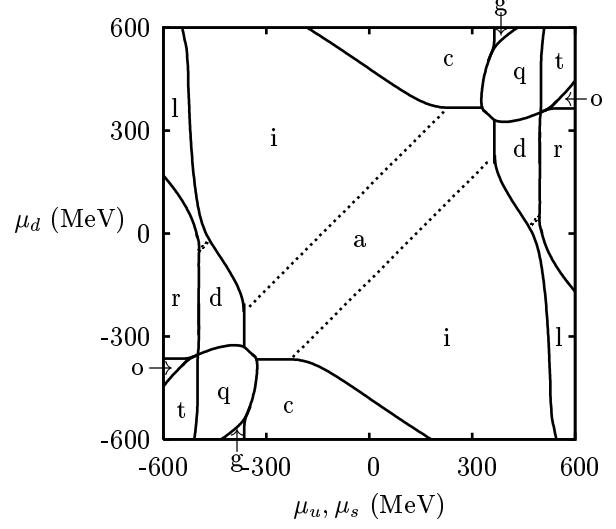


FIG. 5: Phase diagram for  $T = 0$  as a function of  $\mu_u = \mu_s$  and  $\mu_d$ . First and second-order transitions are indicated by solid and dotted lines, respectively. The letters denote the different phases, where a:  $\bar{u}u + \bar{d}d + \bar{s}s$ , c:  $\bar{u}u + \bar{s}s$ , d:  $\bar{d}d + \bar{s}s$ , g:  $\bar{s}s$ , i:  $\pi^+/\pi^- + \bar{s}s$ , l:  $K^0/\bar{K}^0$ , o: 2SCus, q: 2SC +  $\bar{s}s$ , r: 2SCus +  $\bar{d}d$  and t: CFL.

In Fig. 6, we show the phase diagram as a function of  $\mu_d$  and  $T$ , for fixed  $\mu_u = \mu_s = 550$  MeV. In this figure one can find five critical points. Also, one can see in this figure that the  $K^0/\bar{K}^0$  phase (l) is separated from the 2SCus phase (r) by a first-order transition for all temperatures. Furthermore, it is interesting that at finite temperature there is a first-order transition from the phase in which the neutral kaons condense (l) to the pion condensed phase (h). In Fig. 7, we have enlarged the lower-right corner of Fig. 6 for clarity. In this figure one can find all possible superconducting phases, including the more exotic uSC (u), dSC (v) and sSC (w) phases. For  $\mu_u = \mu_d = \mu_s$  one goes from the CFL phase (t) via the 2SC phase (n) to the chirally restored phase when raising the temperature. However, small differences between  $\mu_u = \mu_s$  and  $\mu_d$  can cause one to go through completely different phases.

## V. CONCLUSIONS

In this paper, we studied the phase diagram of the three-flavor NJL model including pseudoscalar condensation and color superconductivity as a function of the different quark chemical potentials and temperature. The NJL model has a rich and interesting phase structure. The pseudoscalar condensed and color superconducting phases are competing and are separated by a first-order phase transition. As we have discussed, this need not be the case for other (less conventional) choices of the parameters of the model.

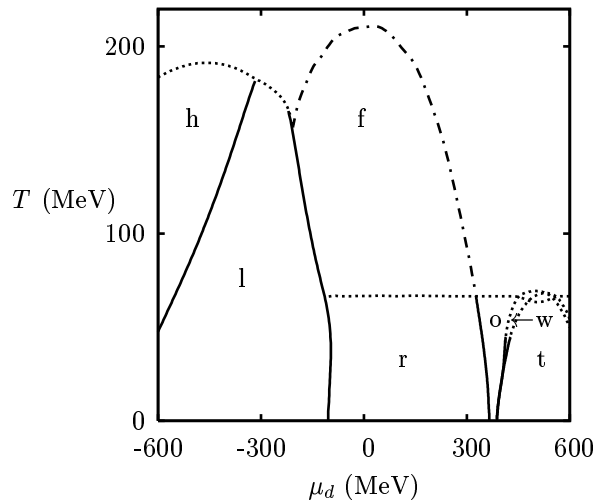


FIG. 6: Phase diagram as a function of  $\mu_d$  and  $T$ , for fixed  $\mu_u = \mu_s = 550$  MeV. First and second-order transitions are indicated by solid and dotted lines, respectively, while cross-overs are denoted by dashed-dotted lines. The uppermost phase without label is the restored phase. The letters denote the different phases, where f:  $\bar{d}d$ , h:  $\pi^+/\pi^-$ , l:  $K^0/\bar{K}^0$ , o: 2SCus, r: 2SCus +  $\bar{d}d$ , t: CFL and w: sSC. The lower right corner of this figure is enlarged in Fig. 7.

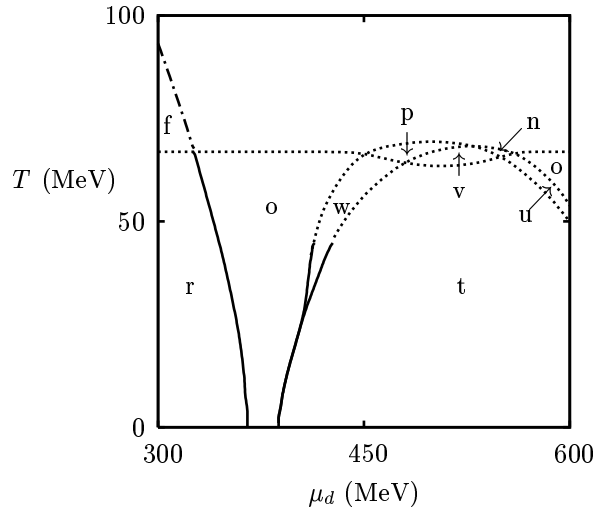


FIG. 7: Same as Fig. 6. The phases that occur are f:  $\bar{d}d$ , n: 2SC, o: 2SCus, p: 2SCds, r: 2SCus +  $\bar{d}d$ , t: CFL, u: uSC, v: dSC and w: sSC.

Furthermore, we concluded that at zero temperature and zero strange quark chemical potential, there is a minimum asymmetry of about 35 MeV between the up and the down quark chemical potentials required in order to have two first-order transitions, when going from the phase with spontaneous chiral symmetry breaking to the 2SC phase.

Our results provide a qualitative check and extension of several earlier calculations that appeared in the literature. The new aspects of the phase diagrams are often located in regions, where the quark chemical potentials are large and very different in magnitude for the different flavors. Although such situations are not necessarily realized in compact stars or can be realized in heavy-ion collisions, a comparison with future lattice data may nevertheless provide interesting information. This is especially relevant for pseudoscalar condensation in the phase where chiral symmetry is restored and also for the complicated superconductivity phase structure close to the cutoff of the model.

This work can be extended in several ways. For example, one can take into account 't Hooft's instanton-induced interaction [53]. If one has pseudoscalar condensation, this is more difficult than in the normal case. Another useful extension would be the inclusion of the neutrality conditions [13, 14], in which case the phase structure changes and for instance gapless phases will occur. It would also be interesting to see how the results depend on the strength of the diquark coupling and also on the quark masses. Furthermore, one could add the LOFF phase [45]. In this crystalline phase, quarks of different momenta can pair. One could also include vector interactions. In this case spin-1 diquark condensation (see for example Refs. [54, 55]) and an induced Lorentz-symmetry breaking (ISB) phase [56] are among the possibilities. It would also be worthwhile to take pseudoscalar diquark condensation [34] into account. Finally, one could try to go beyond the mean-field approximation as was done in Ref. [57].

## Acknowledgments

The research of D.B. has been made possible by financial support from the Royal Netherlands Academy of Arts and Sciences.

[1] F. Karsch, E. Laermann and A. Peikert, Phys. Lett. B **478**, 447 (2000).  
[2] Z. Fodor and S. D. Katz, JHEP **0203**, 014 (2002).  
[3] P. de Forcrand and O. Philipsen, Nucl. Phys. B **642**, 290 (2002).  
[4] C. R. Allton *et al.*, Phys. Rev. D **66**, 074507 (2002).  
[5] M. D'Elia and M. P. Lombardo, Phys. Rev. D **67**, 014505 (2003).

[6] M. A. Halasz, A. D. Jackson, R. E. Shrock, M. A. Stephanov and J. J. M. Verbaarschot, Phys. Rev. D **58**, 096007 (1998).  
[7] J. Berges and K. Rajagopal, Nucl. Phys. B **538**, 215 (1999).  
[8] D. Bailin and A. Love, Phys. Rept. **107**, 325 (1984).  
[9] M. G. Alford, K. Rajagopal and F. Wilczek, Phys. Lett. B **422**, 247 (1998).

- [10] R. Rapp, T. Schäfer, E. V. Shuryak and M. Velkovsky, Phys. Rev. Lett. **81**, 53 (1998).
- [11] M. G. Alford, K. Rajagopal and F. Wilczek, Nucl. Phys. B **537**, 443 (1999).
- [12] M. G. Alford, J. Berges and K. Rajagopal, Nucl. Phys. B **558**, 219 (1999).
- [13] M. Alford and K. Rajagopal, JHEP **0206**, 031 (2002).
- [14] A. W. Steiner, S. Reddy and M. Prakash, Phys. Rev. D **66**, 094007 (2002).
- [15] F. Neumann, M. Buballa and M. Oertel, Nucl. Phys. A **714**, 481 (2003).
- [16] M. G. Alford, J. Berges and K. Rajagopal, Phys. Rev. Lett. **84**, 598 (2000).
- [17] I. Shovkovy and M. Huang, Phys. Lett. B **564**, 205 (2003).
- [18] M. Alford, C. Kouvaris and K. Rajagopal, Phys. Rev. Lett. **92**, 222001 (2004).
- [19] M. Alford, C. Kouvaris and K. Rajagopal, Phys. Rev. D **71**, 054009 (2005).
- [20] S. B. Rüster, I. A. Shovkovy and D. H. Rischke, Nucl. Phys. A **743**, 127 (2004).
- [21] H. Abuki, M. Kitazawa and T. Kunihiro, arXiv:hep-ph/0412382.
- [22] S. B. Rüster, V. Werth, M. Buballa, I. A. Shovkovy and D. H. Rischke, arXiv:hep-ph/0503184.
- [23] D. Blaschke, S. Fredriksson, H. Grigorian, A. M. Öztas and F. Sandin, arXiv:hep-ph/0503194.
- [24] B. Klein, D. Toublan and J. J. M. Verbaarschot, Phys. Rev. D **68**, 014009 (2003).
- [25] D. Toublan and J. B. Kogut, Phys. Lett. B **564**, 212 (2003).
- [26] M. Frank, M. Buballa and M. Oertel, Phys. Lett. B **562**, 221 (2003).
- [27] D. T. Son and M. A. Stephanov, Phys. Rev. Lett. **86**, 592 (2001).
- [28] J. B. Kogut and D. Toublan, Phys. Rev. D **64**, 034007 (2001).
- [29] A. Barducci, G. Pettini, L. Ravagli and R. Casalbuoni, Phys. Lett. B **564**, 217 (2003).
- [30] J. B. Kogut and D. K. Sinclair, Phys. Rev. D **66**, 034505 (2002).
- [31] A. Barducci, R. Casalbuoni, G. Pettini and L. Ravagli, Phys. Rev. D **69**, 096004 (2004).
- [32] A. Barducci, R. Casalbuoni, G. Pettini and L. Ravagli, Phys. Rev. D **71**, 016011 (2005).
- [33] D. Blaschke, M. K. Volkov and V. L. Yudichev, Eur. Phys. J. A **17**, 103 (2003).
- [34] M. Buballa, Phys. Lett. B **609**, 57 (2005).
- [35] T. Schäfer, Phys. Rev. Lett. **85**, 5531 (2000).
- [36] P. F. Bedaque and T. Schäfer, Nucl. Phys. A **697**, 802 (2002).
- [37] D. B. Kaplan and S. Reddy, Phys. Rev. D **65**, 054042 (2002).
- [38] R. Casalbuoni and R. Gatto, Phys. Lett. B **464**, 111 (1999).
- [39] D. T. Son and M. A. Stephanov, Phys. Rev. D **61**, 074012 (2000).
- [40] R. Casalbuoni, Z. y. Duan and F. Sannino, Phys. Rev. D **62**, 094004 (2000).
- [41] M. M. Forbes, arXiv:hep-ph/0411001.
- [42] Y. Nambu and G. Jona-Lasinio, Phys. Rev. **122**, 345 (1961).
- [43] S. P. Klevansky, Rev. Mod. Phys. **64**, 649 (1992).
- [44] M. Buballa, Phys. Rept. **407**, 205 (2005).
- [45] M. G. Alford, J. A. Bowers and K. Rajagopal, Phys. Rev. D **63**, 074016 (2001).
- [46] D. Weingarten, Phys. Rev. Lett. **51**, 1830 (1983).
- [47] E. Anderson et. al., LAPACK User's Guide, Third Edition. SIAM, Philadelphia, (1999).
- [48] F. James and M. Roos, Comput. Phys. Commun. **10**, 343 (1975).
- [49] P. F. Bedaque, Nucl. Phys. A **697**, 569 (2002).
- [50] L. He, M. Jin and P. Zhuang, arXiv:hep-ph/0503272.
- [51] F. Gastineau, R. Nebauer and J. Aichelin, Phys. Rev. C **65**, 045204 (2002).
- [52] S. Lawley, W. Bentz and A. W. Thomas, arXiv:nucl-th/0504020.
- [53] G. 't Hooft, Phys. Rev. D **14**, 3432 (1976).
- [54] R. D. Pisarski and D. H. Rischke, Phys. Rev. D **61**, 074017 (2000).
- [55] M. Buballa, J. Hosek and M. Oertel, Phys. Rev. Lett. **90**, 182002 (2003).
- [56] K. Langfeld and M. Rho, Nucl. Phys. A **660**, 475 (1999).
- [57] J. Hüfner, S. P. Klevansky, P. Zhuang and H. Voss, Annals Phys. **234**, 225 (1994).